Assembly of Partially Oxidized Tetrathiafulvalene in Layered Phosphates. Formation of Conducting Organic−Inorganic Hybrids by Intercalation†

Rénal Backov, Bernard Bonnet, Deborah J. Jones, and Jacques Rozière*

Laboratoire des Agrégats Moléculaires et Matériaux Inorganiques, ESA CNRS 5072, Université Montpellier II, Place E. Bataillon, 34095 Montpellier Cedex 5, France

Received February 10, 1997. Revised Manuscript Received June 4, 1997⊗

Intercalation and ion-exchange reactions have been used for the synthesis of novel inorganic−organic hybrid materials comprised of tetrathiafulvalene (TTF) conducting chains interleaved with insulating zirconium phosphate layers. Two different synthetic strategies are described. In the first approach, we have attempted the oxidative insertion of neutral TTF into a $Zr(PO_4)(HPO_4)_2{\cdot}2H_2O$ host preexchanged with Cu^{2+}. In the second method, surfactant or long-chain alcohols have been used to expand the layers of the host structure, allowing the intercalation of partially charged TTF molecules. This latter approach produced materials with metal-like conductivity that exceeds by a factor of 10^7 that of the precursors. These compounds have been characterized by vibrational, UV−vis, and EPR spectroscopies, and transport properties (conductivity and thermoelectrical power) have been measured as a function of the temperature from −150 to 50 °C. The properties observed show marked similarity with those displayed by mixed valence TTF halides and pseudohalides. The reactions occur topotactically, and the increase in interlayer distance is compatible with an orientation of TTF perpendicular, or nearly, to the host layers.

1. Introduction

Compounds having a two-dimensional structure provide a specific environment that can be used for the spatial organisation or confinement of organic molecules.[1] The nature of the guest, its concentration, the charge density, and electron-transfer properties of the host layers are factors decisive in the conception of new materials. Polymer layered host nanocomposites[2] are just one example of the growing family of hybrid organic inorganic materials derived from layered solids.[3]

It was first recognized some 15 years ago that layered solids could be used to provide the means of separating stacks of organic π-donor molecules,[4] emulating the organization often observed in organic metals prepared in a one-step reaction.[5] The best examples to date are provided by bis(ethylenedithio)tetrathiafulvalene−FeOCl[6] and by TTF−$FePS_3$[7] systems, which have room-temperature conductivities of 0.26 and 3 S cm^{-1}, respectively. In general, the use of a redox-active host matrix can be considered to restrict the range of materials that can be prepared insofar as the reaction between a structural ion and TTF is "all or nothing", since there is no control over the ultimate partial oxidation state of TTF. The aims of the study presented here were to make use of techniques of intercalation chemistry—ion exchange, preexpansion, exfoliation and flocculation around a guest ion, etc.—so as to both assemble and spatially organize partially oxidized $TTF^{\delta+}$ within the interlayer gallery of an appropriate inorganic host while, at the same time, exercising a degree of control over the extent of electron transfer.

Zirconium phosphate (ZrP) is a well-known layered solid which crystallizes in two forms known as α and γ. These differ in the structural arrangement in the layers, the surfaces carrying O_3POH groups in the former[8a,b] and $O_2P(OH)_2$ groups in the latter.[8c,d] α-structured metal(IV) phosphates have, in particular, been exten-

† Dedicated to Professor Dr. Walter Siebert on the occasion of his 60th birthday.

⊗ Abstract published in *Advance ACS Abstracts,* July 15, 1997.

(1) (a) *Intercalation Chemistry*; Whittingham, M. S., Jacobson, A. J., Eds.; Academic Press: New York, 1982. (b) Schöllhorn, R. *Chem. Mater.* **1996**, *8*, 1747. (c) Costantino, U. *Inorganic Ion Exchange Materials*; Clearfield, A., Ed.; CRC Press: Boca Raton, FL, 1982; pp 111−132. (d) *Comprehensive Supramolecular Chemistry*; Alberti, G., Bein, T., Eds.; Pergamon: New York, 1996; Vol. 7.

(2) (a) Ding, Y.; Jones, D. J.; Maireles-Torres, P.; Rozière, J. *Chem. Mater.* **1995**, *7*, 562. (b) Costantino U.; Marmottini, F. *Mater. Chem. Phys.* **1993**, *35*, 193. (c) Wang, Z.; Lan, T.; Pinnavaia, T. J. *Chem. Mater.* **1996**, *8*, 2200. (c) Hutchinson, J. C.; Bissessur, R.; Shriver, D. F. *Chem. Mater.* **1996**, *8*, 1597. (d) Wu, C.-G.; DeGroot, D. C.; Marcy, H. O.; Schindler, J. L.; Kannewurf, C. R.; Liu, Y.-J.; W. Hirpo, Kanatzidis, M. G. *Chem. Mater.* **1996**, *8*, 1992. (e) Messersmith, P. B.; Giannelis, E. P. *Chem. Mater.* **1993**, *5*, 1064. (f) Aranda, P.; Ruiz-Hitzky, E. *Chem. Mater.* **1992**, *4*, 1395. (g) Yanagisawa, T.; Yokoyama, C.; Kuroda, K.; Kato, C. *Bull. Chem. Soc. Jpn.* **1990**, *63*, 47. (h) Mehotra, V.; Giannelis, E. P. *Solid State Ionics* **1992**, *51*, 115. (i) Ruiz-Hitzky, E. *Adv. Mater.* **1993**, *5*, 334.

(3) O'Hare, D. *New J. Chem.* **1994**, *18*, 989.

(4) (a) Antonio, M. R.; Averill, B. A. *J. Chem. Soc., Chem. Commun.* **1981**, 382. (b) Bringley, J. F.; Averill, B. A.; Fabre, J.-M. *Mol. Cryst. Liq. Cryst.* **1988**, *170*, 215. (c) Van Damme, H.; Obrecht, F.; Letellier, M. *Nouv. J. Chim.* **1984**, *8*, 681. (d) Averill B. A.; Kauzlarich, S. M. *Mol. Cryst. Liq. Cryst.* **1984**, *107*, 55.

(5) (a) Munakata, M.; Kuroda-Sowa, T.; Maekawa, M.; Hirota, A.; Kitagawa, S. *Inorg. Chem.* **1995**, *34*, 2705. (b) Inoue, M. B.; Inoue, M.; Bruck, M. A.; Fernando, Q. *J. Chem. Soc., Chem. Commun.* **1992**, 515. (c) Pénicaud, A.; Boubekeur, K.; Batail, P.; Canadell, E.; Auban-Senzio, P.; Jérome, D. *J. Am. Chem. Soc.* **1993**, *115*, 4101. (d) Batail, P.; Boubekeur, K.; Fourmigué, M.; Dolbecq, A.; Gabriel, J.-C.; Guirauden, A.; Livage, C.; Uriel, S. *New. J. Chem.* **1994**, *18*, 999. (e) Geiser, U.; Wang, H. H.; Donega, K. M.; Anderson, B. A.; Williams, J. M.; Kwak, J. F. *Inorg. Chem.* **1986**, *25*, 401. (f) Urayama, H.; Yamochi, H.; Saito, G.; Nozawa, K.; Sugano, T.; Kinoshita, M.; Sato, S.; Oshima, K.; Kawamoto, A.; Tanaka, J. *Chem. Lett.* **1988**, 55.

(6) (a) Bringley, J. F.; Fabre, J.-M.; Averill, B. A. *J. Am. Chem. Soc.* **1990**, *112*, 4577. (b) Bringley, J. F.; Fabre, J.-M.; Averill, B. A. *Chem. Mater.* **1992**, *4*, 522.

(7) Léaustic, A.; Audière, J. P.; Lacroix, P. G.; Clément, R.; Lomas, L.; Michalowicz, A.; Dunham, W. R.; Francis, A. H. *Chem. Mater.* **1995**, *7*, 1103.

S0897-4756(97)00083-5 CCC: $14.00

sively used in the recent past for the assembly of inorganic[9] and organic[1c,10] species. Both are known as ion-exchangers and materials appropriate for the insertion of basic molecules and polymers and as media for interlayer reactivity, properties that are based on proton-transfer characteristics of the hydrogen phosphate. Although the acid protons of zirconium phosphate have been shown to oxidize neutral molecules such as cobaltocene,[11] electron-transfer properties can be more readily induced by making use of the above ion-exchange characteristics to preinsert a redox center into the interlayer region, in an approach first developed for the intercalative redox polymerization of aniline.[12]

We describe below two original methods for the insertion/formation of partially charged TTF in layered zirconium phosphates. The first of these is based on the use of varying amounts of the ion-exchange capacity of γ-ZrP for Cu(II) to create an oxidizing precursor matrix then used in reaction with neutral TTF. It allows the degree of charge transfer and amount of inserted TTF to be directly related to the associated electrical properties, and preliminary results have been briefly reported.[13] In the second method, long-chain alcohols and surfactants have been used to expand the interlayer distance and increase the hydrophobicity of the interlayer region, so facilitating insertion of partially charged TTF. The choice of a specific expanding agent enables modulation of the proportion of protons transferred or exchanged, so defining an effective ion-exchange capacity for the modified zirconium phosphate precursor. This approach leads to materials that have by far the highest conductivity of any phase based on zirconium phosphate.

2. Experimental Section

2.1. Synthesis. γ-$ZrPO_4{\cdot}H_2PO_4{\cdot}2H_2O$ (γ-ZrP) and α-$Zr(HPO_4)_2{\cdot}H_2O$ (α-ZrP) were synthesized according to the methods described by Alberti.[14,15]

Precursor Phases. Cu(II) exchanged forms were prepared by suspending γ-ZrP (0.2 g) in an aqueous solution of $Cu(OAc)_2$ (100 mL, 0.005−0.0125 mol dm^{-3}) to give γ-$ZrPO_4{\cdot}(H_{2-2x}PO_4)$-$Cu_x{\cdot}nH_2O$ with $x = 0.035$, 0.11, 0.21, 0.33, and 0.50 and $n =$ 2−4 (Cu determined by atomic absorption spectroscopy and water content by thermogravimetric analysis).

γ-$ZrPO_4{\cdot}[HO(CH_2)_7CH_3)]_{0.87}(H_2PO_4){\cdot}1.22H_2O$ was prepared by contacting the solid (1 g) with octanol (100 mL) in a closed vessel for 24 h with stirring. Powder X-ray diffraction (XRD) indicated expansion to 29.0 Å and TGA analysis effected rapidly after centrifugation confirmed the above composition.

α-$Zr(H_{1-x/2}PO_4)_2[(H_3C)_3N(CH_2)_{11}CH_3]x{\cdot}1.3H_2O$, $x = 0.65$−0.8. Expansion of α-ZrP with trimethyldodecylammonium (TMDDA) ion cannot be achieved by direct ion exchange. α-ZrP (1 g) was preexpanded by contact overnight with propylamine vapor (50 mL, closed vessel), and the propylammonium ion exchanged in a second stage for TMDDA (dispersion of 1 g of $[Zr(PO_4)_2(CH_3CH_2CH_2NH_3)_2]$ in a solution of 4 g of TMDDABr in 200 mL of ethanol/water 1/1 v/v). Over several syntheses, single-phase materials of interlayer spacing 20−26 Å were obtained containing 0.6−0.8 TMDDA/Zr.

Synthesis of $(TTF)_3(BF_4)_2$.[16] TTF (0.875 g) was dissolved in acetonitrile (30 mL) and a solution of 48% aqueous fluoroboric acid (0.542 g) and 30% hydrogen peroxide (0.162 g; addition of hydrogen peroxide to ice-cold fluoroboric acid) was added. On cooling over an ice-bath, the solution afforded black crystals. $(TTF)_3(BF_4)_2$ (784) calcd: C 27.6, H 1.53, S 49.0%. Found: C 28.1, H 1.64, S 49.7%. $(TTF)_3(BF_4)_2$ contains both fully ionized and neutral TTF in its structure.[17]

Synthesis of $TTFBr_{0.76}$.[18] A stoichiometric amount of Br_2 in CH_3CN (1.22 mol dm^{-3}) was added dropwise to a solution of TTF (0.5 g) in CH_3CN (100 mL). The violet-black precipitate was recovered on a glass frit and washed with acetonitrile. $TTFBr_{0.76}$ was separated from any other bromide salts by recrystallization in warm ethanol. The violet crystals which precipitated from the red-violet ethanol solution gave a single Raman line at 1444 cm^{-1}, corresponding to the presence of $TTF^{0.76+}$ (see below).

Insertion of TTF^+. γ-ZrP (0.2 g) or α-ZrP−TMDDA (0.2 g) was dispersed in solution of $(TTF)_3(BF_4)_2$ in acetonitrile (0.3 mol dm^{-3}, 50 mL) and stirred at 40 °C for 6 days. The solid was recovered by centrifugation, washed, and dried. γ-$ZrPO_4$-$(H_{1.2}PO_4)(TTF)_{0.80}{\cdot}2H_2O$ (480) calcd: C 11.9, H 1.38, S 21.2%. Found: C 11.9, H 1.73, S 21.3%. α-$Zr(H_{0.65}PO_4)_2{\cdot}(TTF)_{0.7}{\cdot}1.1H_2O$ (446) calcd: C 11.1, H 1.43, S 20.1%. Found: C 12.5, H 1.63, S 21.4%.

Insertion of TTF. All manipulation was performed under flowing nitrogen.

Insertion in Cu(II)-Exchanged Phases. A TTF solution (acetonitrile, 0.03 mol dm^{-3}, 50 mL) was added to samples of γ-$ZrPO_4{\cdot}(H_{2-2x}PO_4)Cu_x{\cdot}nH_2O$ (0.1 g) dispersed in acetonitrile (30 mL). After stirring at 40 °C for 6 days, the solid phase was recovered by centrifugation, washed, and dried.

Insertion in γ-ZrP−Octanol and α-ZrP−TMDDA. The precursor phase of ZrP (α or γ, 0.3 g) was dispersed in a solution of TTF (1 g, 0.004 89 mol) in ethanol (200 mL) with stirring. A stoichiometric amount of bromine in acetonitrile (0.002 44 mol of Br_2 mL^{-1}) was added drop by drop over a period of 6 h, with gentle heating to 40 °C. The coffee-colored solid phase was then recovered by centrifugation and washed three times with 50 mL volumes of ethanol/acetonitrile.

2.2. Characterization. Host α- and γ-ZrP and all intercalation compounds derived from them were characterized by powder X-ray diffraction (XRD) using a Philips generator (Cu Kα radiation) and goniometer. Elemental (CHS) analysis was performed using an Erba Science 1108 instrument, and analysis for Cu (both before and after the insertion reaction with TTF) used atomic absorption spectrometry (AAS). Thermogravimetric (TGA) and differential thermal analyses (DTA) were carried out in air on a Stanton Redcroft STA 781 thermobalance. The heating rate was 2 °C min^{-1}. Infrared spectra were recorded in transmittance mode at room temperature on KBr disks using a Bomem DA8 FTIR spectrometer. Raman spectra were obtained either on pressed disks using grazing incidence or on powders contained within a thin-walled capillary tube and spun in a rotating cell, with a Spectraphysics Ar laser ($\lambda = 514.5$ nm) and Dilor spectrometer. Use of higher energy lines (488.0 nm) leads to rapid degradation of all samples by progressive oxidation of $TTF^{\delta+}$ as seen

(8) (a) Clearfield, A.; Smith, G. D. *Inorg. Chem.* **1969**, *8*, 431. (b) Albertsson, J.; Oskarsson, A.; Tellgren, A.; Thomas, J. O. *J. Phys. Chem.* **1977**, *81*, 574. (c) Christiansen, A. N.; Krogh Andersen, A.; Krogh Andersen, I. G.; Alberti, G.; Nielsen, M.; Lehmann, M. S. *Acta Chem. Scand.* **1990**, *44*, 865. (d) Poojary, D. M.; Shpeizer, B.; Clearfield, A. *J. Chem. Soc., Dalton Trans.* **1995**, 111.

(9) (a) Olivera-Pastor, P.; Maireles-Torres, P.; Rodríguez-Castellón, E.; Jiménez-López, A.; Cassagneau, T.; Jones, D. J.; Rozière, J. *Chem. Mater.* **1996**, *8*, 1759. (b) Clearfield, A. In *Multifunctional Mesoporous Inorganic Solids*; Sequeira, C. A. C., Hudson, M. J., Eds.; NATO ASI; Kluwer Academic: Dordrecht, 1993; Vol. 400, pp 159−178.

(10) (a) Alberti, G.; Casciola, M.; Costantino, U.; Vivani, R. *Adv. Mater.* **1996**, *8*, 291. (b) Clearfield, A. *Curr. Opin. Solid State Mater. Sci.* **1996**, *1*, 268. (c) Garcia, M. E.; Naffin, J. L.; Deng, N.; Mallouk, T. E. *Chem. Mater.* **1995**, *7*, 1968.

(11) Johnson, J. W. *J. Chem. Soc., Chem. Commun.* **1980**, 263.

(12) Jones, D. J.; El Mejjad, R.; Rozière, J. *Supramolecular Architecture: Synthetic Control in Thin Films and Solids*; Bein, T., Ed.; *ACS Symp. Ser.* **1992**, *499*, 220−230.

(13) Backov, R.; Jones, D. J.; Rozière, J. *J. Chem. Soc., Chem. Commun.* **1996**, 599.

(14) Alberti, G.; Bernasconi, M. G.; Casciola, M. *Reactive Polym.* **1989**, *11*, 245.

(15) Alberti, G.; Torracca, E. *J. Inorg. Nucl. Chem.* **1968**, *30*, 317.

(16) Wudl, F. *J. Am. Chem. Soc.* **1975**, *97*, 1962.

(17) Legros, J.-P.; Bousseau, M.; Valade, L.; Cassoux, P. *Mol. Cryst. Liq. Cryst.* **1983**, *100*, 181.

(18) La Placa, S. J.; Corfield, P. W. R.; Thomas, R.; Scott, B. A. *Solid State Commun.* **1975**, *17*, 635.

Table 1. Oxidative Insertion of TTF in Cu^{2+}-Exchanged γ-ZrP: Effect of the Stoichiometry of the Precursor Phase on the Uptake of TTF and Its Charge

mol of preexchanged Cu^{II} $ZrH_{2-2x}Cu_x(PO_4)_2 \cdot yH_2O$[a]	charge on TTF[b]	empirical formula[c]	relationship Cu^{II} exchanged TTF insertion and charge[d]	conductivity at 25°C/S cm^{-1}
0.035	0.78	$Zr(PO_4)_2(TTF)_{0.1}(H)_{1.92} \cdot 0.9H_2O$	1.11	$10^{-3.5}$
0.11	0.90	$Zr(PO_4)_2(TTF)_{0.24}(H)_{1.78} \cdot 0.9H_2O$	0.98	$10^{-3.6}$
0.21	0.94	$Zr(PO_4)_2(TTF)_{0.46}(H)_{1.57} \cdot 1.1H_2O$	1.03	$10^{-3.9}$
0.33	0.96	$Zr(PO_4)_2(TTF)_{0.75}(H)_{1.28} \cdot 0.9H_2O$	1.09	$10^{-3.9}$
0.5	0.98	$Zr(PO_4)_2(TTF)_{1.05}(H)_{1.0} \cdot 1.9H_2O$	1.03	$10^{-4.5}$

[a] From atomic absorption spectrometry. [b] From Raman spectroscopy. [c] From elemental analysis C, H, S. [d] TTF content × partial charge/meq Cu(II) in precursor = $bc/2a$. The expected value of d is 1.

by the displacement to lower wavenumbers of the position of the line corresponding to the ν(C═C) mode of TTF, which is sensitive to the degree of charge transfer on the ion. Transmission UV−vis−NIR spectra were recorded on KBr disks between 310 and 2500 nm on a Varian spectrometer. Direct current electrical conductivity and thermopower measurements were performed on pressed disks (thickness 0.5 mm). Conductivity measurements were made between −180 and 80 °C using the "four-point method" of Van der Pauw and fine (50 μm) gold needles for the current and voltage electrodes. Thermoelectric power was measured from −140 to 25 °C using a slow ac technique and copper electrodes. Electron spin resonance (4−298 K) spectra were recorded using a Bruker ER 200D spectrometer operating at 9 GHz (X-band).

3. Results and Discussion

3.1. Assembly of TTF under Controlled Oxidation Conditions. Direct ion exchange of TTF^+ from a solution of $(TTF)_3(BF_4)_2$ occurs with protons of the $(HO)_2PO_2$ groups of γ-ZrP, giving a new compound of interlayer distance 19.7 Å. TGA and elemental analysis concur to provide a formula of $ZrPO_4(H_{1.2}PO_4)(TTF)_{0.80} \cdot 2H_2O$. Facile exchange also takes place with α-ZrP−TMDDA to give α-$Zr(H_{0.65}PO_4)_2 \cdot (TTF)_{0.7} \cdot 1.1H_2O$ of basal spacing 15 Å.

When α- or γ-ZrP is contacted with a solution containing neutral TTF, however, neither ion exchange nor acid−base mechanisms can operate, and no reaction occurs. Nevertheless, oxidative intercalation becomes possible with neutral TTF if the γ-ZrP matrix is preexchanged with Cu(II). The exchange of Cu(II) into γ-ZrP has been studied by Clearfield.[19] He showed that the system is mono- or biphasic, depending on the degree of copper loading, although the interlayer distance is invariant, 12.4 Å. In this work, γ-$ZrPO_4 \cdot (H_{2-2x}PO_4)Cu_x \cdot nH_2O$ with $x = 0.035$, 0.11, 0.21, 0.33, and 0.50 and $n = 2-4$ was used, the second and third of these samples lying in the biphasic region. Figure 1 shows the XRD patterns of γ-ZrP, γ-$ZrPO_4 \cdot (H_{2-2x}PO_4)Cu_x \cdot nH_2O$ and the material recovered after redox ion exchange with TTF. The interlayer distance observed, independent of the copper content of the precursor, is 19.7 Å, identical with that given by materials prepared by direct ion exchange with TTF^+. The expansion of 10−11 Å corresponds to the long dimension of the TTF molecule and so may indicate an orientation with the long axis perpendicular to the plane of the ZrP sheets; this point is addressed in greater detail in section 3.3.

The results of chemical analyses of the products of the redox ion-exchange reaction are given in Table 1. It is noted that no copper could be detected in any of the products after reaction with TTF. Copper is therefore reduced and eliminated, presumably as colloidal Cu^0.

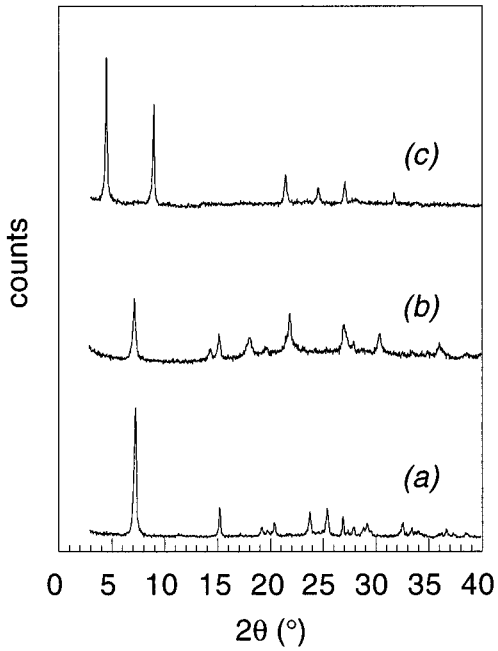

Figure 1. XRD patterns of (a) γ-ZrP, (b) γ-$ZrPO_4 \cdot (H_{2-2x}PO_4)Cu_x \cdot nH_2O$, (c) γ-$Zr(PO_4)_2H_{2-nz}(TTF^{n+})z \cdot H_2O$.

The stoichiometries of Table 1 derived from analytical data show that the amount of TTF inserted in copper-exchanged γ-ZrP closely depends on the degree of copper loading of the precursor phase, with precursors of low copper loading leading to phases containing little TTF, and vice versa. Moreover, the copper content of the precursor influences also the degree of oxidation of inserted TTF as determined by Raman spectroscopy and described below. The equation for the reaction may then be written

$$\gamma\text{-}ZrPO_4 \cdot (H_{2-2x}PO_4)Cu_x \cdot nH_2O + z\,TTF\ (soln) \rightarrow \gamma\text{-}Zr(PO_4)_2H_{2-nz}(TTF^{n+})z \cdot H_2O + x\,Cu^0$$

and the number of meq of Cu(II) in precursor Cu(II)-exchanged γ-ZrP is equal to the product of the partial charge, n^+, on the TTF taken up, z.

The positions of bands and lines in the vibrational spectra of TTF are sensitive to its degree of partial charge. The position of the stretching vibration ν(C═C) in Raman spectroscopy is particularly useful, since it has been shown to vary linearly between 1520 cm^{-1} for the neutral molecule and 1415 cm^{-1} for the fully ionized species.[20] For the intercalated zirconium phosphates, only the compound prepared by direct ion exchange with TTF^+ gave a signal corresponding to the presence of a

(19) Clearfield, A.; Kalnins, J. M. *J. Inorg. Nucl. Chem.* **1978**, *40*, 1933.

(20) Matsuzaki, S.; Moriyama, T.; Toyoda, K. *Solid State Commun.* **1980**, *34*, 857.

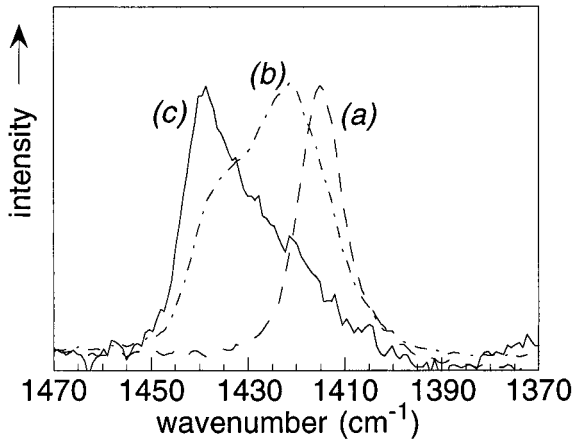

Figure 2. Raman spectra of TTF^+ (a) and of redox intercalates obtained using Cu(II)-exchanged precursors with $x = 0.21$ (b) and 0.035 (c). Partial charges are 1+, 0.94+, and 0.78+, respectively.

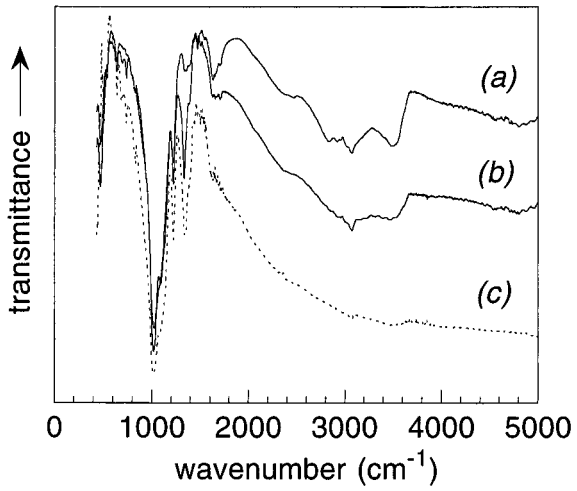

Figure 3. IR spectra of TTF^+ (a) and of redox intercalates obtained using Cu(II)-exchanged precursors with $x = 0.21$ (b) and 0.035 (c). Partial charges are 1+, 0.94+, and 0.78+, respectively.

fully ionized species, all those prepared via Cu(II)-exchanged precursors are characterized by the presence of partially oxidized TTF (Figure 2). For example, for γ-$ZrPO_4 \cdot (H_{2-2x}PO_4)Cu_x \cdot nH_2O$ with $x = 0.035$, the line at 1440 cm^{-1} indicates the presence of TTF with partial oxidation state 0.78, and for that with $x = 0.21$ (biphasic precursor), the Raman line is asymmetric, with a maximum at 1422 cm^{-1} and a shoulder at 1438 cm^{-1}, positions which correspond to charges of 0.94+ (dominant) and 0.78+ (minor; Table 1). At loadings higher than ca. 0.4 Cu/Zr, almost complete oxidation of TTF occurs.

The IR spectra (Figure 3) are superpositions of bands arising from the inorganic matrix and from intercalated TTF. Two factors are worthy of particular comment. First, that the spectral baseline is significantly affected by increasing absorption toward high frequencies, due to a band of maximum at ca. 4900 cm^{-1}. Materials for which the lowest degree of charge transfer to TTF has occurred give IR spectra having greatest increasing background absorption, evidence for an increasing presence of charge-transfer stacks (see below). Second, the intensity of the IR absorption at 1340 cm^{-1} increases inversely with the partial charge on TTF (and hence inversely with the TTF content of the intercalate). This vibration corresponds to the IR component of the ν(C=C) mode and its enhanced intensity, which has also been reported for the MPS_3/TTF system,[21] originates in a vibronic interaction with the mixed-valence charge-transfer transition seen in NIR.[22]

The electrical resistivity was measured using the four-point technique. The use of gold electrodes ensured that any transport properties observed result from electronic rather than ionic (protonic) charge carriers. The polarization effect was monitored by applying the dc current over an extended period of time (no change observed over 30 min). The use of disks of compacted powder provides a value for the electronic conductivity which is averaged over all crystallographic directions, although anisotropy of electrical properties is to be expected. The resistivities observed are clearly a function of the degree of charge transfer and of TTF content of the intercalates. Thus the compound prepared by direct ion exchange with TTF^+ has conductivity of $10^{-5.5}$ S cm^{-1}, whereas materials prepared by redox ion exchange are increasingly less resistive as the initial Cu(II) content of the precursor phase decreases. The most conductive phase has a conductivity of $10^{-3.5}$ S cm^{-1}, a 100-fold increase. There is therefore a direct relationship between the degree of copper loading on γ-ZrP, the subsequent uptake of TTF and its partial charge, and the electronic conductivity. The lowest partial charge on TTF gives the most highly conducting phase, which suggests, given the limited uptake under these conditions (0.1 TTF/Zr), that $TTF^{0.78+}$ must be stacked in islets sufficiently close to allow orbital overlap. The conductivity of this material still lies, however, in the semiconductor range. Any further increase requires the low partial charge on TTF to be maintained, while increasing the TTF uptake. Such a result seems difficult to achieve using the redox intercalation method, in view of the observed interchange between the Cu(II) content, TTF uptake, and partial charge. This led us to develop the approach described below designed to separate the electron transfer and insertion reactions into consecutive steps.

3.2. Assembly of $TTF^{0.72+}$ in α-ZrP and γ-ZrP. *3.2.1. X-ray Diffraction, Chemical, and Thermal Analysis.* In the precursor phases the interlayer distance is consistent with a double layer of octanol molecules in γ-ZrP ($d_{002} = 29.0$ Å) and a single layer of TMDDA ions in α-ZrP ($d_{002} = 22.6$ Å). For the latter, the intercalation reaction could be achieved only by ion exchange with propylammonium, while for the former the driving force for the reaction is probably hydrogen-bond formation with the protons on the internal layers. The stoichiometry of these precursor phases is limited by the covering effect to α-$Zr(H_{1.30}PO_4)_2[(H_3C)_3N(CH_2)_{11}CH_3]_{0.70} \cdot 1.3H_2O$ (α-ZrP−TMDDA) and, for intercalation of octanol, by the ion-exchange capacity of γ-ZrP to γ-$ZrPO_4 \cdot [HO(CH_2)_7CH_3)]_{0.87}(H_2PO_4) \cdot 1.2H_2O$ (γ-ZrP−octanol). Reaction of TTF oxidized in situ by bromine with preexpanded phases of α- and γ-ZrP leads to materials in which the interlayer distance, given by the d_{002} diffraction line, is lowered in each case compared with that of its immediate precursor. Thus γ-ZrP−octanol gives a TTF-inserted phase of interlayer distance 19.4 Å, and α-ZrP−

(21) Miyazaki, T.; Matsuzaki, S.; Ichimura, K.; Sano, M. *Solid State Commun.* **1993**, *85*, 949.
(22) Bozio, R.; Zanon, I.; Girlando, A.; Pecile, C. *J. Chem. Phys.* **1979**, *71*, 2282.

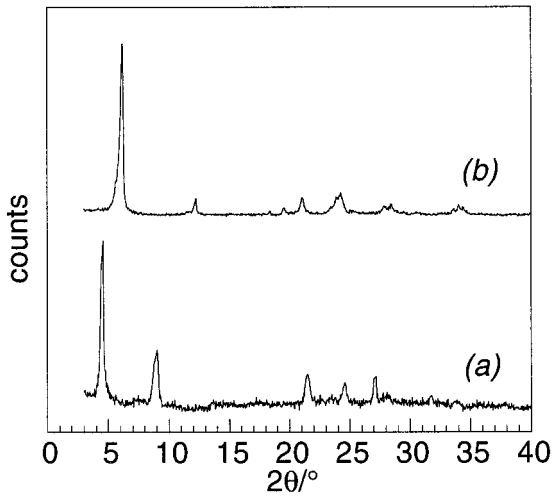

Figure 4. XRD patterns of γ-ZrP−$(TTF^{0.72+})_{1.22}$ (a) and α-ZrP−$(TTF^{0.72+})_{0.93}$ (b).

TMDDA to a compound of interlayer spacing 14.3 Å (Figure 4). The results of chemical analyses and TGA are in good agreement and indicate compositions of α-$Zr(PO_4)_2H_{1.33}TTF^{0.72+})_{0.93}\cdot 1.2H_2O$ [α-ZrP−$(TTF^{0.72+})_{0.93}$] and γ-$ZrPO_4\cdot(H_{1.1}PO_4)(TTF^{0.72+})_{1.22}\cdot 1.2H_2O$ [γ-ZrP−$(TTF^{0.72+})_{1.22}$], where the partial charge on TTF was determined from the position of the ν(C═C) line in Raman spectroscopy (see section 3.2.2). TGA shows water to be lost up to 150 °C, while TTF is then eliminated in two distinct stages below 550 °C, with a change in rate of loss of TTF at ca. 375 °C.

3.2.2. Vibrational and UV−Vis−NIR Spectroscopy. The Raman spectra of TTF-intercalated phases prepared by insertion from Br_2-oxidized TTF solutions show a single line in the region 1400−1550 cm^{-1} with a maximum at 1447 cm^{-1}. This position corresponds to a partial oxidation state of 0.72+, in the range reported for salts prepared by bromine oxidation of TTF in ethanol, $TTFBr_{0.71-0.76}$.[20] Compared with the spectra of Figure 2, where the compounds were prepared by redox intercalation with a Cu(II)-containing matrix, the Raman line is less broad and more symmetrical, inferring that the TTF species inserted has a rather limited range of, or indeed a unique, partial charge.

As for γ-ZrP−$TTF^{\delta+}$ prepared via Cu(II) exchanged phases, IR spectra of α-ZrP−$(TTF^{0.72+})_{0.93}$ and γ-ZrP−$(TTF^{0.72+})_{1.22}$ show the formally IR-inactive ν(C═C) stretch at 1360 cm^{-1}, and a strikingly broad absorption which increases in intensity from 1600 to 5000 cm^{-1}. This feature is notably absent from either of the precursors γ-ZrP−octanol or α-ZrP−TMDDA and is a direct result of the presence of intercalated $TTF^{0.72+}$.

Figure 5 shows the UV−vis−NIR spectra over the range 4000−32000 cm^{-1} (2500−310 nm; 0.5−4.0 eV) given by α-ZrP−$(TTF^{0.72+})_{0.93}$ and γ-ZrP−$(TTF^{0.72+})_{1.22}$. Four absorption peaks are observed, with maxima near 4600, 12400, 18400, and 25100 cm^{-1} (0.57, 1.54, 2.28, and 3.11 eV) for γ-ZrP−$(TTF^{0.72+})_{1.22}$. A slight shift of the broad band in the NIR region to higher energies ($\Delta\nu$ = 200 cm^{-1}) is observed for α-ZrP−$(TTF^{0.72+})_{0.93}$. Using the notation of Torrance[23] developed for mixed-valence TTF halides, these features will be referred to as bands A−D, respectively. Bands C and D are intramolecular

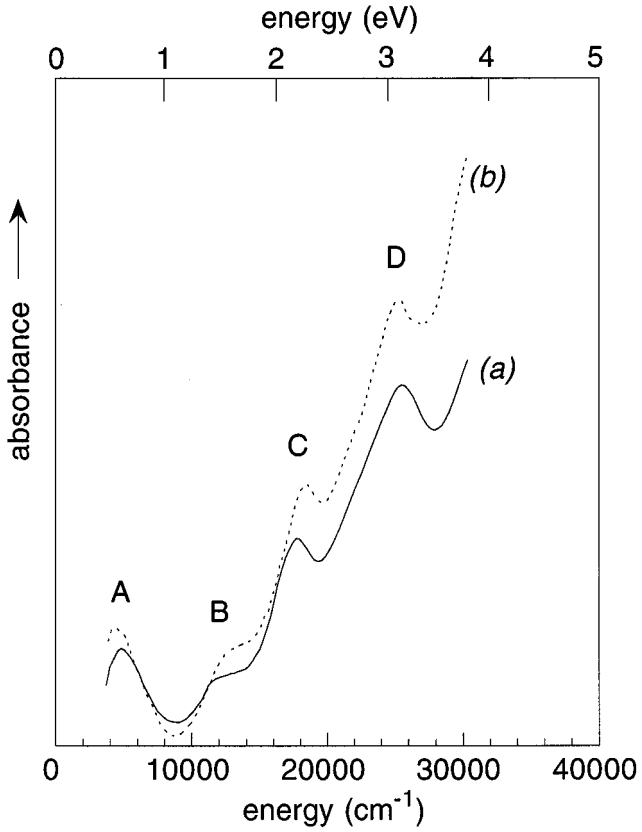

Figure 5. UV−vis−NIR spectra of γ-ZrP−$(TTF^{0.72+})_{1.22}$ (a) and α-ZrP−$(TTF^{0.72+})_{0.93}$ (b).

excitations of charged TTF which are generally observed for both monovalence and mixed valence salts of TTF. Their maxima are shifted to higher frequency when TTF is not structurally isolated, as for $(TTF^+)_2$ or in $TTFBr_{0.79}$. Bands C and D are observed at positions close to those reported for this latter compound. At lower energy, B and A are charge-transfer bands, and A described as a mixed-valence charge-transfer band, due to the presence of mixed valence stacks. The presence of this peak, which is the origin of the continuum seen in IR, has been related to the high dc conductivity of organic metals.[23]

3.2.3. Transport Properties. Four probe electrical conductivity measurements were made on pressed pellets of powdered samples over the temperature range −150 to 30 °C. The room-temperature conductivity recorded for various preparations of α-ZrP−$(TTF^{0.72+})_{0.93}$ and γ-ZrP−$(TTF^{0.72+})_{1.22}$ lies between 3 and 5 S cm^{-1}, significantly above that of any other intercalation compound derived from ZrP.[24] Most interestingly, the temperature dependence of the conductivity is different for the two compounds. Near 25 °C, γ-ZrP−$(TTF^{0.72+})_{1.22}$ behaves as a metallic conductor, its conductivity increasing slowly as the temperature is lowered. Over the same range, the conductivity of α-ZrP−$(TTF^{0.72+})_{0.93}$ is still weakly thermally activated, suggesting that this phase has metal-like semiconductor behavior. Furthermore, a plot of the logarithm of the conductivity of γ-ZrP−$(TTF^{0.72+})_{1.22}$ as a function of temperature shows a distinct hump, indicative of a phase transition, at 235 ± 10 K (Figure 6). Below 230 K, the conductivity of both $TTF^{0.72+}$ intercalates drops rapidly, with a thermal

(23) Torrance, J. B.; Scott, B. A.; Welber, B.; Kaufman, F. B.; Seiden, P. E. *Phys. Rev. B* **1979**, *19*, 730.

(24) Pillion, J. E.; Thompson, M. E. *Chem. Mater.* **1991**, *3*, 779.

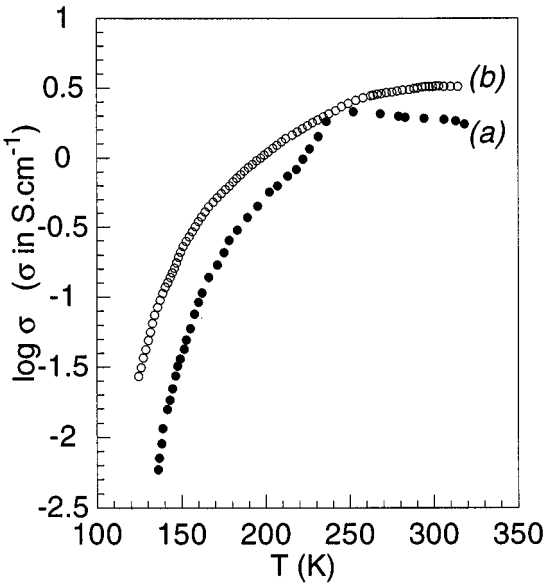

Figure 6. Electrical conductivity of $TTF^{0.72+}$ intercalates. log σ vs T for γ-ZrP−$(TTF^{0.72+})_{1.22}$ (a) and α-ZrP−$(TTF^{0.72+})_{0.93}$ (b).

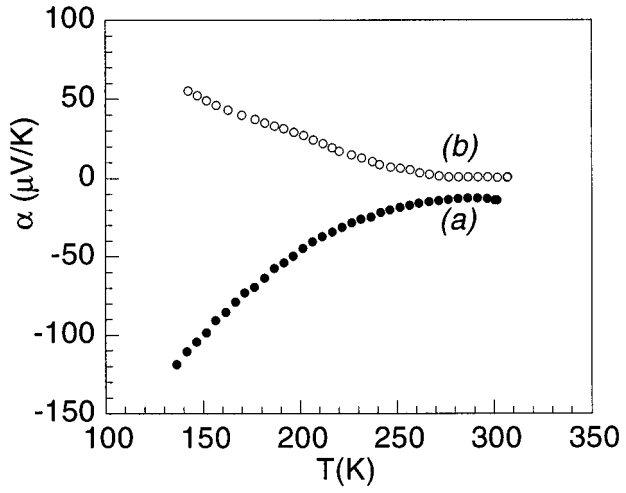

Figure 7. Temperature dependence of Seebeck coefficient of γ-ZrP−$(TTF^{0.72+})_{1.22}$ (a) and α-ZrP−$(TTF^{0.72+})_{0.93}$ (b).

activation similar to that observed for mixed-valence TTF halides.[25,26] Attempts were made to fit the conductivity data to hopping models based on 2- or 3-dimensional hopping, but the results were inconclusive due to the limited temperature range of the data.

The electrical behavior has been further characterized by thermoelectric power measurements (Figure 7). The small negative value of the Seebeck coefficient of γ-ZrP−$(TTF^{0.72+})_{1.22}$, −13 μV K^{-1} at 25 °C, and its slightly negative temperature dependence near room temperature, suggest an n-type metal-like behavior. At lower temperature, the thermopower becomes strongly negative, characteristic of a semiconducting gap. Different behavior is observed for the TTF intercalate derived from α-ZrP, where the Seebeck coefficient is slightly positive at room temperature, 0.061 μV K^{-1}, and shows

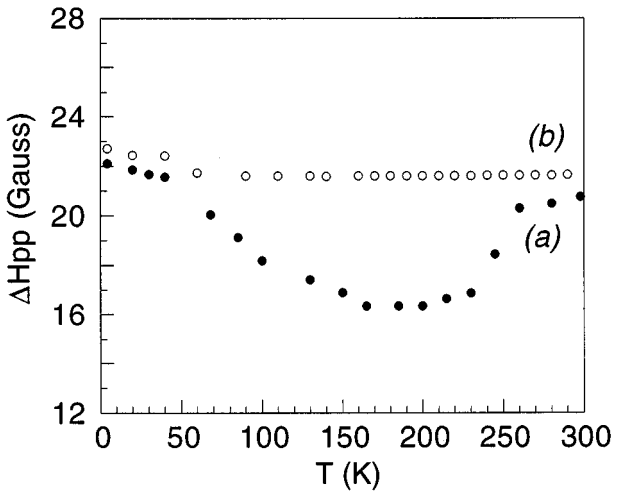

Figure 8. Temperature dependence of EPR line width of γ-ZrP−$(TTF^{0.72+})_{1.22}$ (a) and α-ZrP−$(TTF^{0.72+})_{0.93}$ (b).

a marked upturn at 275 K and then almost linear dependence on temperature down to 150 K. Opposing sign and temperature dependence has also been observed for other, apparently closely related, systems, notably the mixed-valence TTF halides, where $TTFBr_{0.76}$[26] shows the characteristics of an n-type semiconductor, while $TTFI_{0.71}$[25] has p-type and metallic behavior.

3.2.4. Electron Paramagnetic Resonance. Splitting of the EPR signal into two distinct absorption lines is observed for both compounds, even at room temperature, and persists down to the lowest temperature measured (∼4 K). Since spectra were recorded on nonaligned samples, the splitting might arise simply from anisotropic g values. At 300 K, $g_{\parallel}$ and $g_{\perp}$ are 2.0040(5) and 2.0088(5) for γ-ZrP−$(TTF^{0.72+})_{1.22}$ [2.0039-(5) and 2.0089(5) at 87 K] and 2.0030(3) and 2.0079(3) for α-ZrP−$(TTF^{0.72+})_{0.93}$, in good agreement with values given by other mixed valence salts of TTF.[27]

Despite the similarity between the room-temperature line widths of both compounds (22−23 G), their temperature dependence is quite different (Figure 8). Whereas the line width of α-ZrP−$(TTF^{0.72+})_{0.93}$ shows practically no variation in the range 4−300 K, that of γ-ZrP−$(TTF^{0.72+})_{1.22}$ decreases steeply below 250 K, a temperature close to the transition temperature observed in the log σ vs T plot of Figure 6. The line width then gradually broadens again below 150 K to regain its room-temperature value of 22 G at 4 K.

3.3. Discussion. The synthesis of electronically conducting ZrP phases by redox insertion depends on the ability of the Cu(II)-exchanged matrix to assemble partially charged TTF species. The results described in section 2.1 and summarized in Table 1 demonstrate that this objective is attained only by the use of precursor phases of low Cu(II) loading and within the monophasic region defined by Clearfield.[19] In the range $x = 0.08-0.3$ in γ-$ZrPO_4{\cdot}(H_{2-2x}PO_4)Cu_x{\cdot}nH_2O$, the copper-exchanged phases are biphasic, and above this region, TTF is almost completely oxidized to the 1+ state. Indirectly, information is obtained on the nature of the biphasic character in the intermediate range by reaction of γ-$ZrPO_4(H_{1.58}PO_4)Cu_{0.21}{\cdot}nH_2O$ with TTF. The Raman spectrum of this product (Figure 2b) in the range of the ν(C=C) vibration has two components corre-

(25) (a) Somoano, R. B.; Gupta, A.; Hadek, V.; Datta, T.; Jones, M.; Deck, R.; Hermann, A. M. *J. Chem. Phys.* **1975**, *63*, 4970. (b) Wudl, F.; Schaefer, D. E.; Walsh, W. M., Jr.; Rupp, L. W.; DiSalvo, F. J.; Waszczak, J. V.; Kaplan, M. L.; Thomas, G. A. *J. Chem. Phys.* **1977**, *66*, 377.

(26) Chaikin, P. M.; Craven, R. A.; Etemad, S.; La Placa, S. J.; Scott, B. A.; Tomkiewicz, Y.; Torrance, J. B.; Welber, B. *Phys. Rev. B* **1980**, *22*, 5599.

(27) Tomkiewicz, Y.; Taranko, A. R. *Phys. Rev. B* **1978**, *18*, 733.

sponding to the presence of TTF in partial oxidation states 0.78+ and 0.94+ and probably reflecting the existence of phases in the precursor respectively poorer and richer in copper(II). The monophasic region at low copper loading is limited to $x < 0.08$, under which conditions the amount of TTF oxidized and taken up is low.

In a modification to the synthesis, therefore, we developed a different approach, in which partial oxidation states of TTF known to be stabilized in the bulk state as, e.g., mixed-valence halides $TTFX_{0.69-0.78}$ are preferentially formed and inserted into a preconditioned ZrP matrix. Appropriate precursor phases have an increased interlayer distance and hydrophobicity, and an effective ion-exchange capacity which results from the activation of a proportion of the sites on the ZrP surface (through proton transfer to the guest or hydrogen bonding interactions). The effective ion-exchange capacity of a given precursor should match the overall charge transfer to the TTF units; indeed, the product of stoichiometry and partial charge is 0.67+ in α-ZrP−$(TTF^{0.72+})_{0.93}$, close to that of its immediate precursor α-ZrP-$(TMDDA^{+})_{0.70}$, and the charge × stoichiometry product is 0.87+ in γ-ZrP$(TTF^{0.72+})_{1.22}$, identical with the number of activated sites in γ-ZrP(octanol)$_{0.87}$.

For intercalation reactions occurring topotactically and in the absence of exploitable powder X-ray diffraction patterns, structural interpretation is necessarily speculative. However, the mixed-valence nature of the TTF stacks implies that the organic and inorganic layers are not in register, i.e., maximum occupation of the available surface area is independent of the charge distribution on the layers. The surface area available to inserted TTF then defines the stoichiometry of the phases formed. Considering that the structural features of a layer of TTF stacks in mixed-valence halides[18,28] can be transposed into the interlayer region of zirconium phosphates with an average surface area per $TTF^{0.72+}$ of 27.9 Å^2 (mixed valence bromide[18,28]), the ratio of the occupied surface area/available surface area in γ-ZrP is then 1.25 (27.9/35), rationalizing the experimentally observed stoichiometry. This is an indication that the arrangement of $TTF^{0.72+}$ between the layers of γ-ZrP might indeed be similar to that in $TTFBr_{0.76}$ or $TTFI_{0.71}$, where the long axis of TTF is arranged alternatively perpendicular and parallel ("edge-on") to layers of halide ions, allowing the stacks to develop in the interlayer space. The implication then is that the interlayer distance of γ-ZrP−$TTF^{0.72+}$ should be approximately equal to the sum of the thickness of the layers (9 Å) and the long dimension of TTF, 10.7 Å; in agreement, the observed interlayer distance of γ-ZrP−$(TTF^{0.72+})_{1.22}$ is 19.4 Å. A schematic representation of the possible spatial arrangement in such a hybrid organic−inorganic system is given in Figure 9. At this stage, any orientation of the TTF layers parallel to those of the host matrix can be envisaged. Additional information could be obtained from profile refinement[29] of the diffraction patterns, as previously reported for TTF−FeOCl.

Insertion of TTF into other layered matrixes is accompanied by lesser expansion. Neutron profile refinement of FeOCl−TTF[29] shows TTF to be oriented edge-on, compatible with the 5.7 Å gallery height. Here, as with $FePS_3$,[7] where an identical expansion of 5.7 Å is observed, TTF is inserted via a redox process with metal ions in the layers. Possibly the specific assembly of $TTF^{0.72+}$ in the present case allows the layered structure adopted in $TTF_{0.71-0.78}$ mixed halides to be retained in layered γ-zirconium phosphate. For α-ZrP, the ratio between the surface occupied by TTF and the available surface area (24 Å^2) is 0.86, lower than the observed stoichiometry, 0.93. In addition, the interlayer spacing of 14.3 Å (layer thickness in α-ZrP ca. 6.3 Å) suggests that the TTF stacks make an angle of ca. 50° with the plane formed by zirconium phosphate, in an arrangement that effectively increases the occupation of the ZrP surface per TTF. These factors lead us to consider that the packing of TTF in α-ZrP may involve tilted, end-on TTF ions only.

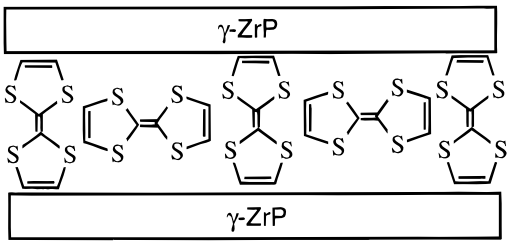

Figure 9. Schematic representation of the proposed arrangement of $TTF^{0.72+}$ in γ-ZrP.

The similarity between mixed-valence TTF halides and zirconium phosphates goes beyond structural factors. The conductivity of both γ-ZrP−$(TTF^{0.72+})_{1.22}$ and $TTFBr_{0.76}$ show a similar dependence on temperature and evidence for a phase transition, although the room-temperature conductivity of ZrP−$(TTF^{0.72+})$ is lower by a factor 3−4 that of compacted powders of $TTFBr_{0.76}$ measured under identical conditions (100 times lower than that of single crystals). In addition, similar values of the Seebeck coefficient are measured for α-ZrP−$(TTF^{0.72+})_{0.93}$ as for $TTFI_{0.71}$,[26] small and positive, and for γ-ZrP−$(TTF^{0.72+})_{1.22}$ as for $TTFBr_{0.76}$,[25a] small and negative.

The synthetic method has the particular advantage of versatility and can probably be generalized to the insertion of partially oxidized TTF in other layered hosts. The use of appropriate precursors allows maximization of the packing density in the interlayer region and control of the oxidation state of TTF. The ZrP−$TTF^{0.72+}$ phases reported here display properties not observed previously in any of the hundreds of ZrP intercalates known. The drawback, of course, is that the preparation of single crystals is precluded, so excluding the evaluation of the expected marked anisotropy of electrical and spectroscopic properties. As a step in this direction, we are currently making use of new methods of exfoliation of ZrP and reprecipitating in the presence of $TTF^{0.72+}$. Self-assembly in this way leads to oriented, and self-supporting films, the full characterization of which will be reported subsequently.

Acknowledgment. We thank Dr. Gérard Brun for his assistance with thermoelectric power measurements. We have enjoyed discussions with Professor Jean-Marc Fabre and Dr. Bernard Mula throughout the course of this work.

CM970083R

(28) Scott, B. A.; La Placa, S. J.; Torrance, J. B.; Silverman, B. D.; Welber, B. *J. Am. Chem. Soc.* **1977**, *99*, 6631.

(29) Kauzlarich, S. M.; Stanton, J. L.; Faber, J., Jr.; Averill, B. A. *J. Am. Chem. Soc.* **1986**, *108*, 7946.